Numerical Modeling for Optimization of the Aspect Ratio of Submerged Vanes for the Purpose of Sediment Deflection in Rivers

V. Chauhan
Shiv Nadar University, vc651@snu.edu.in

R. Chavan
Maulana Azad National Institute of Technology

G. D. Singhal
Shiv Nadar University

Recommended Citation

Chauhan V., Chavan, R., and Singhal, G.D. (2022). "Numerical Modeling for Optimization of the Aspect Ratio of Submerged Vanes for the Purpose of Sediment Deflection in Rivers" in "9th IAHR International Symposium on Hydraulic Structures (9th ISHS)". *Proceedings of the 9th IAHR International Symposium on Hydraulic Structures – 9th ISHS*, 24-27 October 2022, IIT Roorkee, Roorkee, India. Palermo, Ahmad, Crookston, and Erpicum Editors. Utah State University, Logan, Utah, USA, 10 pages (DOI: 10.26077/b079-8746) (ISBN 978-1-958416-07-5).

9th International Symposium on Hydraulic Structures Roorkee, India 24-27 October 2022
ISBN: 978-1-958416-07-5 DOI: https://doi.org/10.26077/b079-8746

Numerical Modeling for Optimization of the Aspect Ratio of Submerged Vanes for the Purpose of Sediment Deflection in Rivers

V. Chauhan[1], R. Chavan[2]&G.D. Singhal[1]
[1]*Shiv Nadar University, Greater Noida, India*
[2]*Maulana Azad National Institute of Technology, Bhopal, India*
E-mail: vc651@snu.edu.in

Abstract: *In order to create a secondary circulation (spiral flow) in the downstream direction to their trailing edge, submerged vanes are tiny aspect ratio (H/L) devices that are positioned vertically on riverbeds. Since this secondary circulation is driven by the vane-induced tip vortex, submerged vanes are best recognized for changing the alluvial river-bed profile. Finding the right aspect ratio as a function of the angle of attack with the approach flow is one of the current issues with using the submerged vane technique. In this context, the current study aims to investigate the best vane length to be used, based on a specific angle of attack with the flow. A pair of rectangular vanes with a set height is among the studied vanes. Only 15^0 and 40^0 angles will be examined in the current study because these are the ideal minimum and maximum recommendations made by earlier studies. The vanes' length to height ratios that were taken into consideration for this investigation were 2, 3, and 4. The purpose of the study is to determine how these variables affect the strength of the secondary circulation and sediment deflection downstream of the vanes. The flow field around and past the submerged vane is investigated using the Flow-3D Hydro numerical model. The most ideal aspect ratios for a low Froude number of 0.168 are 0.25 and 0.33 at 40 and 15 degrees of attack, respectively. The most ideal aspect ratios with a high Froude number of 0.303 are 0.33 and 0.25 at 40 and 15 degrees of attack, respectively.*

Keywords: *inland navigation, morphology, scouring, secondary circulation, sediment deflection, vortex.*

1. Introduction

Small aspect ratio devices called submerged vanes are frequently utilized for river training (Odgaard and Wang 1991b). Sediment deflection is a crucial component of river training due to the increasing amount of sediment entering river systems. To deflect, redirect, and manage the river sediment load, submerged vanes can be used to impart transverse momentum to the approach flow. The vane-induced tip vortex is what causes the transverse momentum. Determining the strength of the tip vortex is therefore essential to assessing the effectiveness of submerged vanes for sediment deflection. The strength of the tip vortex produced by vanes has been measured in existing research using the "moment of momentum" metric (Marelius and Sinha 1998; Gupta et al. 2006; Gupta et al. 2007).

A higher thickness (more than 1mm) is frequently required for a cheaper material to manufacture vanes, but this result in considerably less lift developed per unit area (due to the weir effect), hence a greater length and consequently smaller aspect ratio *(H/L)* is needed for such materials (Odgaard 2009). Since longer vanes produce two or more secondary flow cells instead of just one, they are less efficient (Odgaard and Mosconi 1987). The height of the vane is a crucial design factor for sediment deflection. The length of the vane to be used should be determined by the vane's cost and anticipated effectiveness in managing sediment. Ouyang (2009) suggested a design table to find the ideal vane height at design length of submerged vanes for clear water conditions.

The stress field of the submerged vane extends stream-wise by almost three times the vane height. According to Ouyang (2009), who used their numerical approach, "the difference in performance between a vane height of 0.4 times flow depth and a vane height of 0.65 times flow depth is minimal when either the sediment Froude number or angle of attack is low." These are the desirable effects of vane design since the angle of attack is frequently unstable and subject to fluctuate depending on the design flow and because the vane-induced transverse bed-shear stress tends to carry more bed materials with a higher sediment Froude number. Navigation may also place restrictions on the height of vanes. The height of submerged vanes is therefore kept at 0.4 times the local water depth as an useful rule of thumb. Tan et al. (2005) discovered that for mobile bed conditions, an optimal vane height of two to three times the height of the bed-form can stop the bed-load from "escaping" over the bed-form crest. Additionally, a vane higher than this would severely restrict the flow and hinder sediment mobility; conversely, a vane lower than this would allow bed-load particles to climb over it, decreasing the effectiveness of the vane's sediment deflection. The

highest vortex strength was reported by Gupta et al. (2007) to occur at an aspect ratio of 0.25. They carried out their studies using vanes made of superior material with a thickness of less than 1 cm (Chauhan et al. 2022). To determine the proper aspect ratios for thicker vanes, the current study will use a vane thickness of 5 cm.

The methodologies involved in analytical research of submerged vanes mainly differ with respect to the method used to quantify the vane induced transverse velocity. Odgaard and Spoljaric (1986) used “wing theory” (potential flow method), Marelius and Sinha (1998) used “Moment of Momentum”, Sinha and Marelius (2000) used $k-\epsilon$ turbulence model, Flokstra (2006) used the mathematical model of Odgaard and Wang (1991a) to update morphological modelling system Delft3D-MOR (Struiksma et al. 1985) in order to simulate vane-induced bed level variations and later Ouyang (2009) used “Panel method of aerodynamics”. Gravity causes pressure in an irrotational flow. Pressure develops velocity gradients which in presence of viscosity generates varying shear stress in fluids. Adding these viscous effects to the pressure is always a challenging problem in river mechanics, particularly for the flow around submerged streamlined objects such as submerged vanes. Therefore “Potential flow theory” used by Odgaard and Spoljaric (1986) seems to underperform in comparison to the “Panel Method” in aerodynamics (Chauhan et al. 2022).

Since normal stresses were not adequately represented, Sinha and Marelius' (2000) numerical investigation to solve the three-dimensional Reynold's-averaged Navier-Stokes equations with the turbulence closure as "standard $k-\epsilon$ model" was deemed to have produced unacceptable results. According to Patel and Yoon (1995), the influence of surface roughness can be taken into consideration using the *k-w* turbulence model. To simulate the flow past and around the submerged vanes, the viscous stress tensor in the Navier-Stokes equation can be derived using the k-w turbulence model. The range of possibilities for optimizing the performance of submerged vanes has increased as a result of recent developments in turbulence monitoring and simulation. Previous attempts (Odgaard 1991a; Sinha and Marelius 2000; Flokstra 2006) to create a model for submerged vane performance in sediment deflection did not perform accurately because the potential flow approach served as the theoretical underpinning. The problem has been how to apply the viscous contribution to the pressure in an irrotational flow. The model developed by (Ouyang et al. 2008; Ouyang 2009) is the only one that has been successful in creating a numerical model for submerged vane performance because it more effectively incorporates the effects of bound vortex and combines the viscous contributions to pressure using the Biot-Savart law (Chauhan et al. 2022). Moreover, it is usually advantageous to employ the "moment of momentum" method if the investigation is experimental and focuses on optimizing the vane parameters rather than characterizing them. It is because it is a precise gauge of vortex intensity and is readily quantifiable using turbulence measurements.

Higher angles of attack with the approach flow, such as 40 degrees, have been observed to increase the strength of the tip vortex in the literature (Marelius and Sinha 1998). On the other hand, for angles greater than 15 degrees, the local scouring near submerged vanes also amplifies. Increased local scouring around vanes necessitates deeper installation depths, which is more expensive. Therefore, with regard to approach flow, these two angles of attack—15^0 and 40^0—are the best options for installing vanes. There should be a specific advice to choose the right aspect ratio at these angles of attack because the flow fields obtained with the aforementioned vanes' angles of attack are very different. A recommendation of this kind is being sought to be established in the current investigation. A streamlined "moment of momentum" criterion is used to evaluate the vortex intensity for sediment deflection. The investigation will use two different downstream cross-sections of vanes to measure the 2*D* velocity magnitude of the *y-z* plane. To shed light on the occurrence of local scouring around vanes, the flow field around the vanes will also be examined.

2. Numerical Method

2.1 Governing equations of numerical model

Turbulence in water flow is both unpredictable yet coherent at the same time (Nezu et al. 1993). The experimental measurement of turbulence quantities requires a lot of time and effort. As a result, turbulence models were created in order to associate the turbulence quantities with the flow properties. The Renormalized group (*RNG*) model was used in the current simulation investigation utilizing Flow-3*D* Hydro software. Based on kinetic energy *k* and its rate of dissipation ϵ, the eddy viscosity is calculated using the turbulence closure equations 1 and 2. Because it required less computing than other superior models like the *k-ω* and Large Eddy Simulation (*LES*) model, the adoption of the *RNG* model is preferred. Additionally, it has been noted that the *RNG* model is useful for incorporating the impacts

of vortices and sediment transport. To mimic the changes in bed morphology, we use the Van Rijn equation (Van 1984) of bed load transfer rate.

$$\frac{\partial}{\partial t}(\rho k) + \frac{\partial}{\partial x_i}(\rho k u_i) = \frac{\partial}{\partial x_j}\left(\alpha_k \mu_{eff} \frac{\partial k}{\partial x_j}\right) + G_k + G_b - \rho\epsilon - Y_M + S_k \quad (1)$$

$$\frac{\partial}{\partial t}(\rho \epsilon) + \frac{\partial}{\partial x_i}(\rho \epsilon u_i) = \frac{\partial}{\partial x_j}\left(\alpha_\epsilon \mu_{eff} \frac{\partial \epsilon}{\partial x_j}\right) + C_{1\epsilon}\frac{\epsilon}{k}(G_k + C_{3\epsilon}G_b) - C_{2\epsilon}\rho\frac{\epsilon^2}{k} - R_\epsilon + S_\epsilon \quad (2)$$

Here, G_k = represents the generation of the turbulence kinetic energy due to the mean velocity gradients; G_b= represents the generation of the turbulence kinetic energy due to buoyancy; Y_M = represents the contribution of the fluctuating dilatation in compressible turbulence to the overall dissipation rate; $\alpha_k$and α_ϵ= inverse effective Prandtl numbers for k and ϵ respectively; S_k and S_ϵ = user-defined source terms.

2.2 Model setup

Two separate model setups have been created to simulate two different uniform flow depth settings at a fixed discharge of 0.021 m^3/s. These two model setups were chosen so that they might result in two cases of clear water research and mobile bed study, with Froude numbers of 0.168 and 0.303, respectively. Using Flow-3*D* Hydro's built-in geometry function, the study began by designing the geometries (Fig. 1) for a rectangular open channel bed and submerged vanes. The geometry of the channel bed, which was 0.5 m broad, 5 m long and 0.2 m deep, was classified as "packed sediment." Next, a pair of defined cubical volume submerged vanes was positioned at a set angle of attack with the approach flow. The two "General (Solid)" rectangular vanes in each model setup, with a lateral separation of 10 cm, were positioned in the centre of the created channel geometry. The cubical volume had dimensions of 5 cm in thickness, 0.4*d* in height (where d is the depth of the water), and lengths of 2 × 0.4*d*, 3 × 0.4*d* and 4 × 0.4*d*. Table 1 includes a list of the various model parameters employed in the current study. The submerged vanes model was also used in this work in a variety of geometrical configurations, which are listed in Table 2 along with the relevant designations, geometries, and flow parameters. The table displays 12 alternative submerged vanes configurations that required 12 numerical runs with various model geometries and flow conditions.

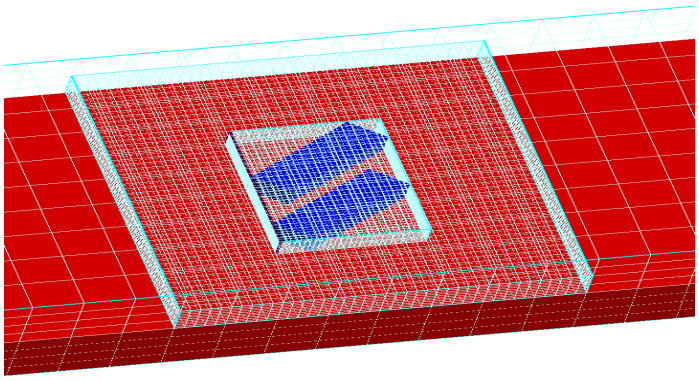

Figure 1. Model and meshing of submerged vanes generated by Flow-3*D* Hydro (*L=2H, α=40⁰ and d=18.5*)

The geometry was made, and then the meshing process was started. With each succeeding decrease in result variation, various mesh sizes were used. The appropriate mesh size is the one "at which the difference in acquired results was less than 5% from the previous coarser mesh size," according to the selection criteria. Based on this standard, the simulation study's mesh sizes were 0.05 m, 0.01 m, and 0.005 m, as shown in Fig.1. To capture the minute flow features at the sharp edges of the vanes, the smallest mesh size is used where the vanes are located. To preserve stability and make sure fluid fraction advection did not exceed computational cell volumes, the time-step size was automatically changed. For all of the taken into consideration geometrical configurations of the submerged vanes, it was discovered that with the 600 s simulation of the flow, the solution became fully converged and the steady state condition was achieved. Using the built-in "*FAVOUR*" feature of the Flow-3*D* Hydro software, the model is evaluated for usability after completion of the geometry and meshing. Then, based on their responsibilities in establishing the underlying physical flow phenomena, boundary conditions were set to each surface of the geometry. A uniform flow boundary condition is imposed for the inlet boundary condition. Initial flow depths at the inlet border are set to 12.5 m and 18.5 m at a discharge value of 0.021 m^3/s. A pressure boundary condition is imposed for the outflow boundary condition. As pressure boundary conditions, 12.5 m and 18.5 m of normal flow

depth were used. The boundary condition "symmetry" is applied to the two *x-z* plane borders. While "atmospheric pressure" is the boundary condition for the highest elevation in the *x-y* plane, "symmetry" is the boundary condition for the lowest elevation. The volume of fluid (*VOF*) method is used to monitor the surface of the water.

Table 1. List of model parameters used in the simulation study

S. No.	Model parameters	Range
1	Width of the channel	0.5 m
2	Length of the channel	5 m
3	Depth of flow	12.5 cm and 18.5 cm
4	Distance between center of vane pair and inlet	2.5 m
5	Height of vane	5 cm and 7.4 cm
6	Thickness of vane	5 cm
7	Length of vane	For 5 cm vane height- 10 cm, 15 cm and 20 cm For 7.4 cm vane height- 14.8 cm, 22.2 cm and 29.6 cm.
8	Angle of attack of vane	15^0 and 40^0
9	Froude number	0.303 (for d = 12.5 cm) and 0.168 (for d = 18.5 cm)
10	Turbulence modeling used	*RNG* model
11	Sediment size (d_{50})	0.0003 m
12	Sediment model	Van Rijn model

Table 2. List of designations for different model configurations with their corresponding geometries and flow parameters used in the simulation study

Designation of *(d. α.L/H)*	Flow depth (d), in cm	Length of vanes (L), in cm	Height of vanes ($H = 0.4d$), in cm	Aspect ratio (H/L)	Angle of attack (α), in degrees	Discharge, in m^3/s	Froude Number
A.1.2	12.5	10	5	0.5	15	0.021	0.303
A.1.3		15		0.33			
A.1.4		20		0.25			
A.2.2		10		0.5	40		
A.2.3		15		0.33			
A.2.4		20		0.25			
B.1.2		14.8		0.5	15		
B.1.3		22.2		0.33			

B.1.4	18.5	29.6	7.4	0.25	40		0.168
B.2.2		14.8		0.5			
B.2.3		22.2		0.33			
B.2.4		29.6		0.25			

2.3 Accuracy of numerical model

The tendencies of changes in transverse velocity in the *z*-direction are in good agreement with the study's experimental findings (Odgaard and Spoljaric 1986). It should be noted that the inclusion of the "weir effect" for the thicker vanes utilized in this study only caused the trends to be similar, although the transverse velocity magnitudes were found to be unequal. It is evident that the magnitude of the transverse velocity has significantly decreased. It is as a result of the model's geometrical features in the current simulation being different from those employed in the experimental study (Odgaard and Spoljaric 1986). Thus, the aspect ratio of submerged vanes was effectively optimized with the help of Flow-3*D* Hydro software.

3. Results and Discussion

The complex velocity patterns produced by the vortices surrounding the vanes help to define the flow field they cause. Without any characterization, the current study's sole goal is to estimate the vortex strength brought on by various vanes' model configurations. To measure and compare the vortex strength among the many configurations used in the current study, a streamlined criterion of "moment of momentum" is applied. Submerged vanes are thought to function better at deflecting sediments when their "moment of momentum" is higher. The magnitude of the velocity perpendicular to the centre of the vortex is precisely proportional to the physical attribute known as "moment of momentum." Therefore, it is hypothesized that the 2*D* velocity magnitudes in the *y*-*z* plane are proportional to the "moment of momentum" and are thus indicative of how well the vane performs in deflecting sediment. Table 3 provides a summary of the simulation findings for the various geometric configurations employed in this investigation. By contrasting the simulation results, vortex strength, local scour, and vane's sediment deflection performance are evaluated and assessed.

3.1 Local scouring around vanes

By contrasting the simulation results of 2-*D* velocity magnitudes in the *y*-*z* plane at the location of vanes, local scouring around vanes is evaluated and assessed. It is determined that the configuration *A.1.2* (Table 3) has excessive local scour while the configuration *B.1.4* has reduced local scour (Fig. 2). This means that at high Froude number values, the larger aspect ratio of 0.5 should be avoided, whereas at low Froude number values, the smaller aspect ratio of 0.25 should be favored. High Froude numbers typically result in more severe local scoring near vanes. Therefore, simply comparing the simulation results for configurations *A.1.4* (Fig. 3) and *A.2.4* (Fig. 4) is used to assess the impact of angle of attack on local scoring. According to Marelius and Sinha (1998), the comparison shows that there are multiple vortex cores immediately downstream of the vanes when the angle of attack is 40 degrees, but only one core is visible when the angle of attack is 15 degrees. Marelius and Sinha (1998) measured the intensity of the tip vortex but ignored its size. The simulation results for the submerged vanes positioned at the 40^0 angle of attack support their contention that there are two suction side vortices and one tip vortex. It appears that the transverse extent of the tip vortex for the vane pair positioned at the 40^0 angle of attack is two times greater than that of the vane pair at the 15^0 angle of attack, which is exhibiting roughly 15 cm of transverse extent of the vortex core. At 40^0, it is displaying a transverse extent of the vortex core of roughly 30 cm. Additionally, the comparison shows that the vane pair oriented at 15^0 has a more coherent vortex. Further analysis of the vortex patterns reveals that the suction side of the vanes installed at the 40^0 angle of attack had more severe local scouring than the vanes installed at the 15^0 angle of attack. Marelius and Sinha (1998) further demonstrated that the horseshoe vortex's extent for vanes positioned at a 40^0 angle of attack reaches toward the suction side in this situation.

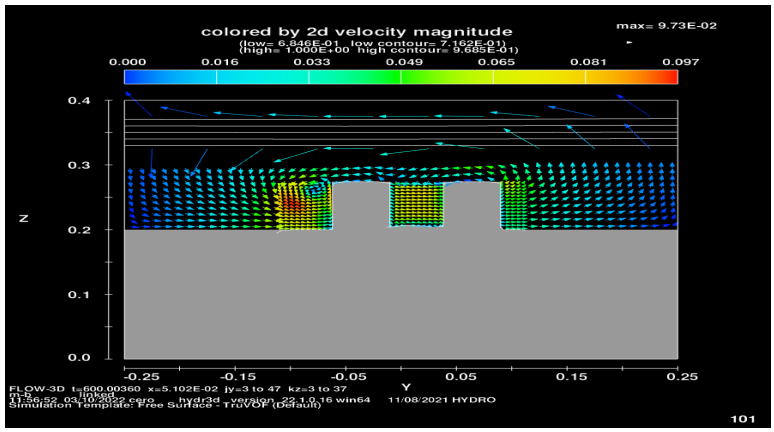

Figure 2. Simulation result to assess local scour at $x = 0$ for the configuration *B.1.4*

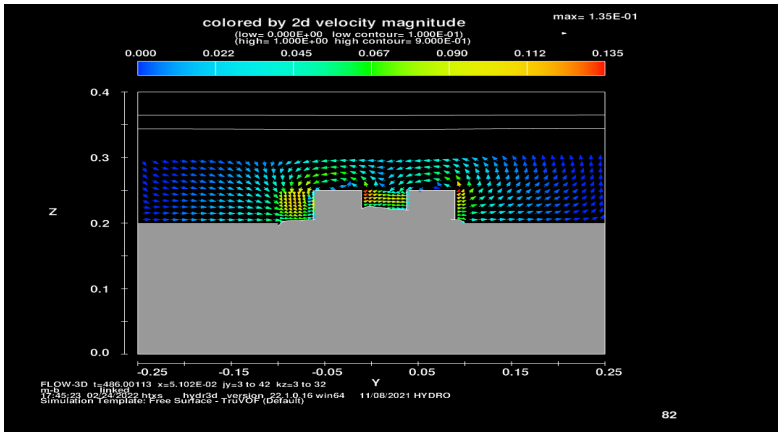

Figure 3. Simulation result to assess local scour at $x = 0$ for the configuration *A.1.4*

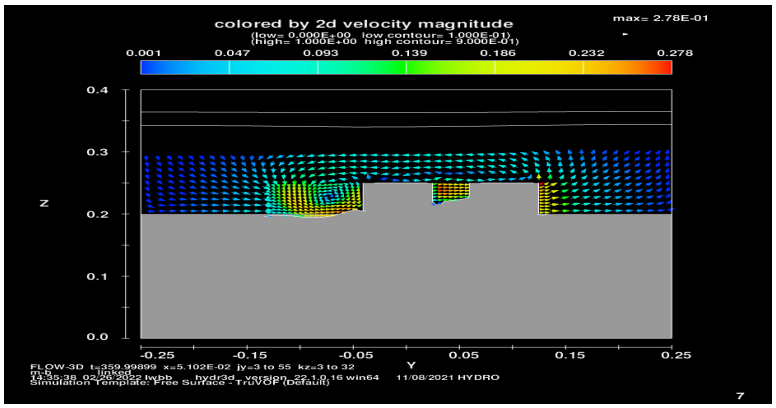

Figure 4. Simulation result to assess local scour at $x = 0$ for the configuration *A.2.4*

3.2 Optimization of aspect ratio based on quantification of local scour and vortex strength

By contrasting the simulation results of the 2-*D* velocity magnitudes in the *y*-*z* plane at two sites downstream from the vanes, the optimization with regard to the vortex strength is carried out. The centre of vane's pair is 5 cm upstream from one of the downstream sites, and the point with the highest 2*D* velocity magnitude in the *y*-*z* plane is the other. In order to provide the comparisons specifically for the various Froude numbers with two extreme angles

of attack, they are divided into the following sections. Comparing several numerical runs demonstrates that installing the vanes at a 40 degree angle of attack, which necessitates deeper installation, is necessary to optimize the performance of sediment deflection. By positioning the vanes at a greater angle of attack with the approach flow, the additional cost of deeper installation should be compensated for.

3.2.1 Lower Froude number value of 0.168

It is determined that an aspect ratio of 0.25 is best to employ at a greater angle of attack of 40 degrees since the best configuration *B.2.4* (Fig. 5) has produced the strongest vortex and the least amount of local scour. An aspect ratio of 0.25 is suitable for lowering scour for an angle of attack as low as 15 degrees, whereas an aspect ratio of 0.33 is preferable to improve the performance of vanes in deflecting sediment. For the 15 degree instance, *B.1.4* (Table 3) and B.1.3 (Fig. 6) are the best geometrical configurations because they reduce scour and improve deflection, respectively. With a tiny aspect ratio of 0.25 and a low Froude number, the vortex must travel further downstream to strengthen. Also, the maximum vortex strength shifts downstream at low Froude numbers when a greater aspect ratio of 0.5 is offered.

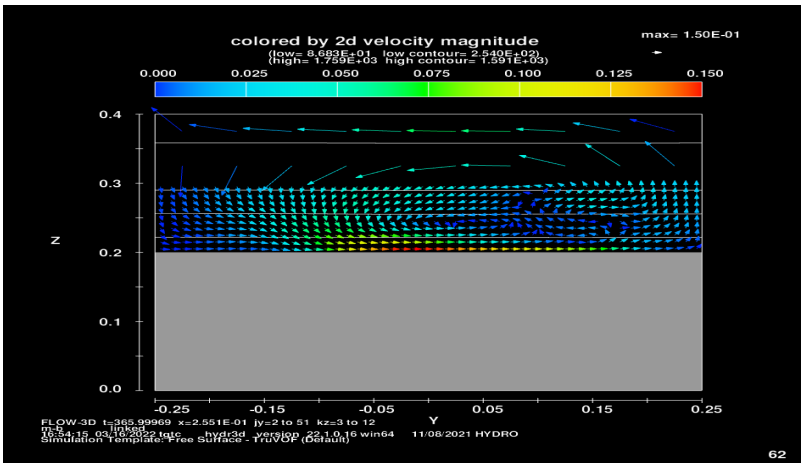

Figure 5. Simulation result at *x = 15* cm for the configuration *B.2.4*

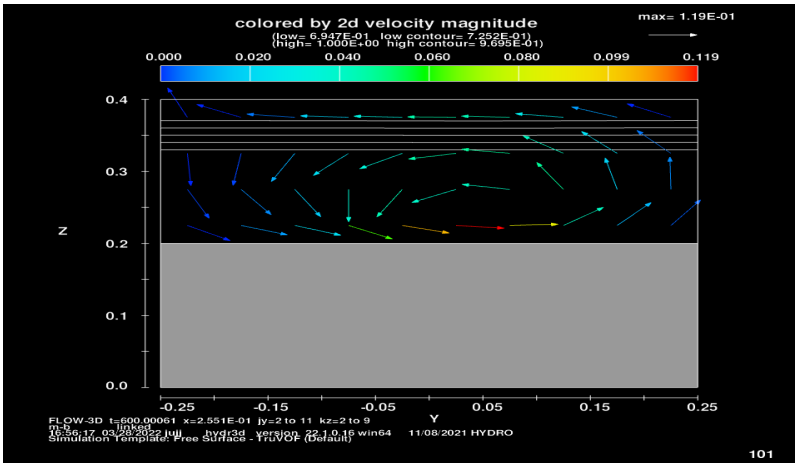

Figure 6. Simulation result at *x = 15 cm* for the configuration *B.1.3*

3.2.2 Higher Froude number value of 0.313

It is determined that an aspect ratio of 0.33 is the most appropriate to adopt at a greater angle of attack of 40 degrees. An aspect ratio of 0.25 is ideal at a lower angle of attack of 15 degrees. They have produced the strongest vortex and the least amount of local scour, therefore this explains why, *A.2.3* (Fig. 7) and *A.1.4* (Fig. 8) are the ideal arrangements for the 40 degree and 15 degree instances, respectively. At a high Froude number and a reduced aspect ratio of 0.25, it is seen that the maximum vortex intensity is shifting downstream. Different bed-forms come into

play as the Froude number rises above the threshold required for the start of sediment motion, and the scouring patterns change quickly within the high Froude number value range. As a result, only when the Froude number is specific to around 0.3 should the results of the current study be considered accurate. Tan et al. (2005) provided a sizable dataset so that researchers could examine how well vanes performed at deflecting sediment over a wider range of Froude numbers in the context of mobile beds.

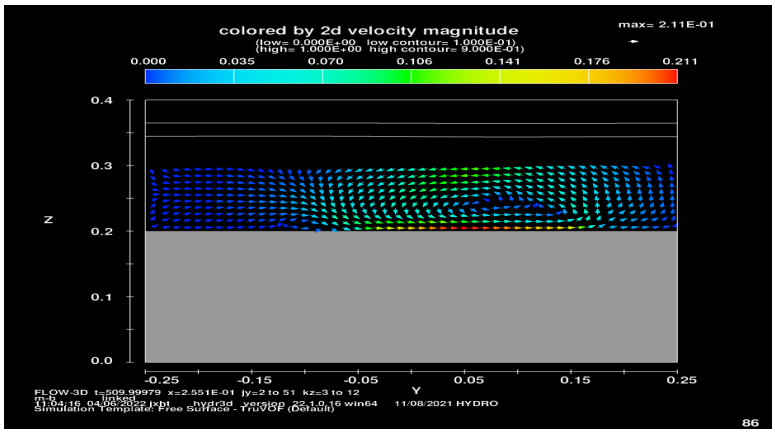

Figure 7. Simulation result at $x = 15$ cm for the configuration *A.2.3*

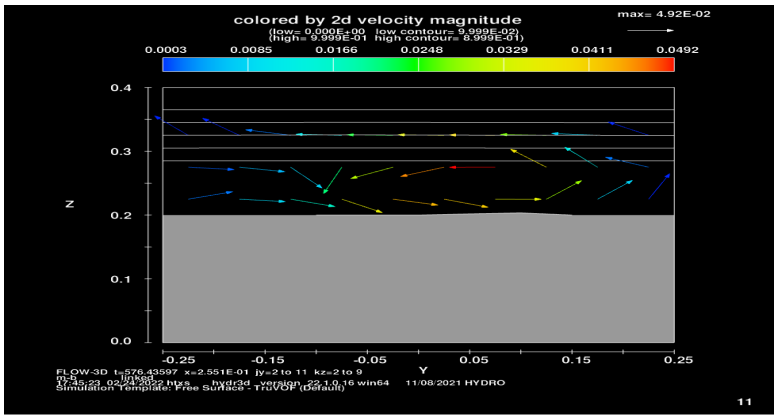

Figure 8. Simulation result at $x = 15$ cm for the configuration *A.1.4*

Table 3. Flow 3D Hydro simulation results for different model configurations used in this study

Designation	Maximum value of 2*D* velocity magnitude in *y-z* plane at $x = 0$ (center of vane's pair), in cm/sec	Maximum value of 2*D* velocity magnitude in *y-z* plane at $x = 5$ cm, in cm/sec	Maximum value of 2*D* velocity magnitude in *y-z* plane between $x = 10$ cm and $x = 250$ cm, in cm/sec
A.1.2	32.2	23.1	4.14
A.1.3	13.7	16.5	4.8
A.1.4	13.5	21	4.92
A.2.2	27.4	18.5	6.02
A.2.3	24.4	25.7	21.1
A.2.4	27.8	26.9	8.7
B.1.2	10.6	11	6.08

B.1.3	11	17.8	11.9
B.1.4	9.7	10.5	10.7
B.2.2	17.7	11.1	5.15
B.2.3	18.6	19.7	9.3
B.2.4	18.2	16.1	15

4. Conclusions

From this numerical study the following conclusions can be made:

1. Comparing the simulation results for the vane pair with an aspect ratio of 0.25 and under high Froude number, it seems that the transverse extent of the tip vortex for the 40^0 angle of attack becomes twice to that in case of the 15^0 angle of attack and also this comparison clearly indicate a more coherent vortex for the vane pair placed at 15 degree.
2. The comparison of vortex patterns also confirmed that the extent of the horseshoe vortex extends towards suction side for the vanes placed at the 40^0 angle of attack and therefore more severe local scouring is observed at the suction side of the vanes placed at the 40^0 angle of attack compared to the vanes at the 15^0 angle of attack.
3. At a low Froude number of 0.168, the most optimum aspect ratios for enhanced sediment deflection are 0.25 and 0.33 at 40 degree and 15 degree angles of attack respectively.
4. For a high Froude number of 0.303, the most optimum aspect ratios for enhanced sediment deflection are 0.33 and 0.25 at 40 degree and 15 degree angles of attack respectively.
5. The larger aspect ratio of 0.5 should be avoided at high Froude number value and smaller aspect ratio of 0.25 should be preferred at low Froude number value

ACKNOWLEDGMENTS

This work was conducted in collaboration with the departments of civil engineering at Shiv Nadar University and Maulana Azad National Institute of Technology.

REFERENCES

1. Chauhan, V., Singhal, G.D. and Chavan, R. (2022). "A review of sediment deflection in rivers using submerged vanes." *ISH J. Hydraul. Eng.*, 1-17.
2. Flokstra, C. (2006). "Modelling of submerged vanes." *J. Hydraul. Research*, *44*(5), 591-602.
3. Gupta, U.P., Ojha, C.S.P. and Sharma, N. (2006). "Vorticity with different shapes of submerged vanes." *ISH J. Hydraul. Eng.*, *12*(1), 13-26.
4. Gupta, U.P., Sharma, N. and Ojha, C.S.P. (2007). "Performance evaluation of aspect ratio of submerged vanes." *Water and Energy International*, *64*(2), 20-26.
5. Marelius, F. and Sinha, S.K. (1998). "Experimental investigation of flow past submerged vanes." *J. Hydraul. Eng.*, *124*(5), 542-545.
6. Nezu, I., Tominaga, A. and Nakagawa, H., 1993. Field measurements of secondary currents in straight rivers. *Journal of Hydraulic Engineering*, *119*(5), pp.598-614.
7. Odgaard, A.J. and Wang, Y. (1991a). "Sediment management with submerged vanes. I: Theory." *J. Hydraul. Eng.*, *117*(3), 267-267.
8. Odgaard, A.J. and Wang, Y. (1991b). "Sediment management with submerged vanes. II: Applications." *J. Hydraul. Eng.*, *117*(3), 284-302.
9. Odgaard, A.J. and Mosconi, C.E. (1987). "Streambank protection by submerged vanes." *J. Hydraul. Eng.*, *113*(4), 520-536.

10. Odgaard, A.J., 2009, April. River training and sediment management with submerged vanes. American Society of Civil Engineers.
11. Ouyang, H.T., Lai, J.S., Yu, H. and Lu, C.H. (2008). "Interaction between submerged vanes for sediment management." *J. hydraul. reserach*, *46*(5), 620-627.
12. Ouyang, H.T. (2009). "Investigation on the dimensions and shape of a submerged vane for sediment management in alluvial channels." *J. Hydraul. Eng.*, *135*(3), 209-217.
13. Patel, V.C. and Yoon, J.Y. (1995). "Application of turbulence models to separated flow over rough surfaces." *ASME.J. Fluids Eng.*, 117(2), 234-241.
14. Sinha, S.K. and Marelius, F. (2000). "Analysis of flow past submerged vanes." *J. of Hydraul. Research*, *38*(1), 65-71.
15. Tan, S.K., Yu, G., Lim, S.Y. and Ong, M.C. (2005). "Flow structure and sediment motion around submerged vanes in open channel." *J. of waterway, port, coastal, and ocean eng.*, *131*(3), pp.132-136.
16. Van Rijn, L.C. (1984). "Sediment transport, part I: bed load transport." *Journal of hydraulic engineering*, *110*(10), 1431-1456.